Exploring Graphene-Based Materials' Genotoxicity: Inputs of a Screening Method.

Salma Achawi [a, b], *Ludovic Huot* [c], *Fabrice Nesslany* [c], *Jérémie Pourchez* [a], *Sophie Simar* [c], *Valérie Forest* [a,*], *Bruno Feneon* [b,*]

[a] Mines Saint-Etienne, Univ Lyon, Univ Jean Monnet, Etablissement Français du Sang, INSERM, U1059 Sainbiose, Centre CIS, F-42023 Saint-Etienne, France.

[b] Manufacture Française des Pneumatiques Michelin, Place des Carmes Déchaux, 63040 Clermont-Ferrand Cedex 9, France.

[c] Genotoxicology Department, Institut Pasteur de Lille, 1, Rue du Professeur Calmette, 59000 Lille, France.

* Corresponding authors :

Valérie Forest: Mines Saint-Etienne, 158 cours Fauriel, CS 62362, 42023 Saint-Etienne Cedex 2. France. Email: vforest@emse.fr

Bruno Feneon: Michelin, 23, Place des Carmes Déchaux 63000 Clermont-Ferrand. France. Email: bruno.feneon@michelin.com

Word count: 5392

Abstract

Graphene-based materials (GBMs) are promising nanomaterials, and several innovations depend on their use. However, the assessment of their potential hazard must be carefully explored before entering any market. GBMs are indeed well-known to induce various biological impacts, including oxidative stress, which can potentially lead to DNA damage. Genotoxicity is a major endpoint for hazard assessment and has been explored for GBMs, but the available literature shows conflicting results. In this study, we assessed the genotoxicity of 13 various GBMs, one carbon black and one amorphous silica through a DNA damage response assay (using a human respiratory cell model, BEAS-2B). Concurrently, oxidative stress was assessed through a ROS production quantification (DCFH-DA assay using a murine macrophage model, RAW 264.7). We also performed a full physicochemical characterization of our samples to explore potential structure-activity relationships involving genotoxicity. We observed that surface oxidation appears linked to genotoxicity response and were able to distinguish several groups within our studied GBMs showing different genotoxicity results. Our findings highlight the necessity to individually consider each nanoform of GBMs since the tested samples showed various results and modes of action. We propose this study as a genotoxicity assessment using a high-throughput screening method and suggest few hypotheses concerning the genotoxicity mode of action of GBMs.

Keywords: Graphene-based materials, genotoxicity, high-throughput screening, structure-activity relationships.

1. Introduction

Graphene-based materials (GBMs) are continuously raising interest since the isolation of graphene in 2004 (Novoselov *et al.* 2004). They include subfamilies such as graphene oxide (GO), reduced graphene oxide (RGO) or graphene nanoplatelets (GNP). Despite their promising properties, the industrial use of GBMs is still minor, and only few of them already led to commercialized innovations. This is partly due to uncertainties concerning their potential risk on human health.

GBMs' toxicity has often been questioned and thoroughly investigated (Fadeel *et al.* 2018). GBMs may indeed trigger various effects: inflammation (Di Cristo *et al.* 2020) or mitochondria physiology imbalance (Jarosz *et al.* 2016) are only few examples. However, GBMs are mostly well-known to induce oxidative stress (Chen *et al.* 2016, Dziewięcka *et al.* 2017, Vranic *et al.* 2018, Ain *et al.* 2019). Genotoxicity is a crucial toxicity endpoint, and two mechanisms can be highlighted: primary genotoxicity is due to the nanomaterial's interaction with target cells whereas secondary genotoxicity involves mechanisms in which nanomaterials do not interact directly with the target cell.

Primary genotoxicity can be direct or indirect. Direct genotoxicity is a consequence of a direct interaction between nanomaterial and DNA or chromosomes by direct binding with DNA or through mechanical effects. It is often considered that direct genotoxicity is a non-threshold effect, supposingly increasing the risk from the smallest dose (Jenkins *et al.* 2010). GBMs such as graphene quantum dots or GO have been shown to be able to penetrate cell nucleus (Wang *et al.* 2010, 2013), a direct contact with nuclear DNA can then be suspected. Some GBMs are known to interact with specific loci of the chromatin (Sun *et al.* 2018). GO, for example, was found to bind directly DNA, which affects the replication process (Liu *et al.* 2013). A direct interaction with DNA can also occur during interphase and may affect replication or transcription mechanisms, which can impact DNA structure and even cause cleavage (Ren *et*

al. 2010). Furthermore, a direct interaction can also be observed between the GBMs and chromosomes during mitosis: in that case, loss of chromosome (aneugenicity) or chromosomal break (clastogenicity) can be observed. Lastly, carbon-based materials are well-known to instrinsically generate free radicals: GBMs are of no exception. Depending on their surface parameters (such as surface oxidation and suface defects), free radicals are released from the GO surface and can directly damage DNA (Dizdaroglu *et al.* 2002).

Indirect genotoxicity does not directly affect DNA but can affect genetic information. GBMs can interact with nuclear proteins involved in the replication, repair or transcription processes (Chatterjee *et al.* 2016). Oxidative stress is defined by the imbalance between pro-oxidants species (including reactive oxygen species, ROS and reactive nitrogen species, RNS) and antioxidants. The increase of ROS is considered to be a major step of the GBMs mode of action and can also indirectly lead to genotoxicity through various mechanisms such as DNA breakage or chromatin remodeling (Tabish *et al.* 2018)(see Figure 1).

8-oxo-dG, an oxidized derivative of deoxyguanosine (one of the deoxyribonucleosides composing DNA), can be formed by the attack of ROS on DNA and has been observed after a GO exposure (Gurunathan *et al.* 2019a, 2019b). When treated with antioxidant (*e.g.*, *N-acetylcysteine*), cells exposed to GBMs show greatly reduced genotoxicity (Burgum, Clift, Evans, Hondow, Tarat, *et al.* 2021). GBMs often present carboxyl groups on their surface which can generate free radicals, eventually inducing genotoxicity (Burgum, Clift, Evans, Hondow, Miller, *et al.* 2021). Other redox-active groups can greatly affect GBMs's oxidative stress and ROS production (Pieper *et al.* 2016). GBMs can also induce mitochondria stress which can also lead to increase the cellular ROS production (Jaworski *et al.* 2019). Moreover, some GBMs can inhibit the antioxidant enzymes (including catalase and superoxide dismutase), which obviously cause an increase in oxidative stress (Deng *et al.* 2019). In physiological conditions and until a certain point, natural cellular mechanisms will compensate this aggression, explaining why

indirect genotoxicity is a thresholded effect. Under a determined threshold, the defense mechanisms are still operational and no adverse effect is actually induced (Kirsch-Volders *et al.* 2003).

Secondary genotoxicity involves mechanisms in which nanomaterials do not interact directly with the target cell but produce an inflammatory response in neighboring cells which will generate ROS/RNS and induce a (secondary) genotoxic effect in the target cell (Evans *et al.* 2017). Hence, secondary genotoxicity is mainly driven by an inflammatory response (Åkerlund *et al.* 2019).

Briefly, aneugenicity, clastogenicity or mutagenicity are major genotoxicity mechanism. For aneugenicity, genotoxicants act primarily on non-DNA targets (microtubule, centrosome or kinetochore (More *et al.* 2021)) or cause damage to the mitosis apparatus, leading to improper chromosome segregation (Parry *et al.* 1996, 2002). For clastogenicity, structural chromosome aberrations such as chromatid/ chromosome breaks occur (Bignold 2009). Clastogenic agents can covalently bind to DNA or enzymes, leading to chromosome breakage. Mutagenicity corresponds to the induction of DNA mutations (Kumar *et al.* 2018), either by direct interaction with DNA or chromatin or by indirect mechanisms, such as through generation of reactive oxygen species or inflammation (DeMarini 2019). Genotoxicity is associated to serious health effects, the first one being cancer (Phillips and Arlt 2009): some genotoxic agents can indeed cause mutations that can eventually lead to malign tumor. Hence, most carcinogenic chemicals are genotoxic (Hayashi 1992), which make the measurement of this endpoint critical for hazard assessment.

The most common *in vivo* genotoxicity assays are chromosome aberration, micronucleus and comet assays (OECD 473, 474 and 489, respectively) (Magdolenova *et al.* 2014). However, in a context of reduction, refinement and replacement of animal testing, and given the considerable number of nanomaterials to be tested, the scientific community is questioning a systematic use

of *in vivo* models, especially considering that *in vitro* genotoxicity assessment can also be reliable when optimized (Corvi and Madia 2017). In the context of a REACH registration of a substance, genotoxicity is currently measured with a mutation test on bacterial system (Ames test, OECD 471) (Stead *et al.* 1981) and an *in vitro* genotoxicity assay on mammalian cell cultures (*e.g.*, gene mutation assay and/or a chromosomal aberrations test). However, it has been demonstrated that the Ames' test is not optimal for nanoforms (Doak *et al.* 2012) and can potentially be replaced by a mutation test on *in vitro* mammal models (OECD guideline 476 or 490). Otherwise, the micronucleus test described in OECD guideline 487 (OECD 2016) is well adapted for nanomaterials but an adaptation is necessary (Gonzalez *et al.* 2011). The increasing number of nanomaterials (Inshakova and Inshakov 2017), is urging us to rethink the methodology of genotoxicity assessment. More and more industries integrate sustainability and safety to their research and development, which implies to consider the use of a safe-by-design approach (Schwarz-Plaschg *et al.* 2017). In this respect, high throughput screening (HTS) genotoxicity testing can present lots of advantages (Sukumaran *et al.* 2016).

Overall, a HTS method provides a quick overview of a toxic mode of action. This implies the coordinated measurement of multiple biomarkers on the same samples. Few DNA damage response (DDR) biomarkers exist and some of them have been thoroughly studied and validated. This is the case of the γH2AX histone (Kopp *et al.* 2019) as well as the H3 histone phosphorylation (Khoury *et al.* 2016, Hamilton *et al.* 2018). γH2AX is sensitive to double strand DNA breakage (Rogakou *et al.* 1998, Bonner *et al.* 2008, Kinner *et al.* 2008) which makes it a biomarker of clastogenicity (Matsuzaki *et al.* 2010), especially when combined with phospho-histone H3 detection (Mishima 2017) which is itself a biomarker of aneugenicity (Wilde *et al.* 2020). γH2AX is also a biomarker of mutagenicity if we consider the repair mechanisms that can be involved after interaction with DNA. The endpoint p53 as an indicator of nuclear p53 may also be investigated. Briefly, p53 is a tumor suppressor and, when a

mutation is detected in a cell, it can stop the cell cycle to trigger DNA repair or induce apoptosis of the cell carrying the mutation. It is a biomarker used for detecting genotoxicity (Bhaskaran *et al.* 1999) or even cancer (Hayman *et al.* 2019). In this paper, we used a HTS method for measuring the genotoxicity impact of a various GBMs. We also studied the relationship between surface oxidation and genotoxicity outcome and discussed potential GBMs genotoxicity mechanisms.

2. Material and Methods

2.1. Nanomaterials

We tested 13 various GBMs. For comparison, we also tested a carbon black and an amorphous silica as reference materials. These samples are depicted in Table 1. Their specific surface area (SSA) was determined by the BET technique (adsorption of nitrogen, with degassing system Micromeritics). Their surface oxidation was determined with XPS (X-ray Photo spectroscopy, Quantera Scanning XPS microprobe, Physical Electronics). Lateral size was determined with electron microscopy (Field Emission Scanning Electron Microscope, from JEOL). The full physicochemical characterization of each of these samples (including ICP analysis, full XPS characterization and RAMAN spectrum) can be found in supplementary data 1.

All nanomaterials were prepared and dispersed in deionized water at 1600 µg/mL as stock solution. Successive dilutions were then prepared in 10% fetal calf serum Dulbecco's Modified Eagle Medium (DMEM, Invitrogen) supplemented with 1% penicillin-streptomycin (Sigma-Aldrich) to obtain the following range of final doses: 100, 75, 50, 37.5, 25, 8.33 and 4.17 µg/cm².

2.2. DDR assay

2.2.1. Cell culture and culture medium

The human bronchial epithelial cell line BEAS-2B was obtained from the American Type Culture Collection (ATCC® CRL-9609™). BEAS-2B cells were seeded at a density of $5x10^5$ cells in 75 cm² Corning® CellBIND® surface cell culture flasks (Corning) and maintained at 37°C in a humidified 5% CO_2 atmosphere in complete Pneumacult Ex-medium (Stemcell), a serum and bovine pituitary extract (BPE)-free cell culture medium. The complete culture Pneumacult Ex-medium contains PneumaCult Ex Basal medium (Stemcell) added by PneumaCult Ex-50X supplement (Stemcell) and hydrocortisone (Stemcell) following the manufacturer's recommendations, antibiotics streptomycin (Streptomycin sulfate salt, Merck) and penicillin (Penicillin G sodium salt, Merck) respectively at 200 UI/mL and 50 µg/mL. Medium was renewed every 2 to 3 days and cells were subcultured before reaching confluence since confluent cultures rapidly undergo squamous terminal differentiation. The doubling time of BEAS-2B cells is approximately 24 hours.

2.2.2. Cell exposure to nanomaterials

A cell suspension at a density of $2x10^5$ cells/mL was prepared in complete Pneumacult Ex-medium. A volume of 100 µL of cell suspension was distributed in 96-well plates CellBIND® surface (Costar) then incubated at 37°C with 5 ± 0.5 % CO_2, 95 ± 5 % humidity. Two treatment schedules were carried out: a 4-hour short-term treatment and a 24-hour continuous treatment. The treatment consisted in replacement of the medium by 200 µL of each dilution of the different nanomaterials prepared in the Complete Pneumacult Ex-treatment medium. Then, the plates were incubated at 37 °C with 5 ± 0.5 % CO2, 95 ± 5 % humidity. Duplicate cell cultures treated with the solvent were used as negative controls. Methylmethane sulfonate (300 µM; Merck, clastogenic substance), vinblastine (24 nM; Merck, aneugenic substance) and griseofulvin (30 µg/mL, Merck, aneugenic substance) were used as positive controls. Please note that for each experiment, a significant genotoxic effect was observed. At the end of the

treatment (4 or 24 hours), the cells were washed by addition of 200 µL PBS1X (Gibco) at 37°C. Then, the washing buffer was replaced by a volume of 50 µL of pre-warmed TrypLE Express (Gibco) at 37°C. Plates were then incubated for 5 minutes at 37°C.

2.2.3. DDR assay protocol

The MultiFlow DNA Damage Kit – p53, γH2AX, Phospho-Histone H3 Kit from Litron Laboratories (product code MultiFlow (p53,γH2AX, H3) ; Rochester, NY 14623, USA) was used. The DDR is a HTS assay that allows the simultaneous measurements of genotoxicity biomarkers (γH2AX and PH3) as well as p53, which can be considered as a biomarker for nuclear translocation. Moreover, the flow cytometry allows to assess cytotoxicity through the nuclei count. Please note that when the nuclei count was considered too low, an additional analysis was performed. Overall, the tested concentration did not induce a major cytotoxicity (the relative nuclei count was largely higher than 50% for moderate doses) on BEAS-2B cells. The experiments were conducted upon the protocol provided by Litron Laboratories, as follows:

***Labelling*:** A volume of 50 µL of the "Complete Labelling Solution" (containing Nuclei Release Solution, Counting Beads, DNA Stain, RNase Solution, filtered FBS and antibodies) was added to individual wells of a clean 96 U-bottom well plate. The cells from the treatment plates were gently resuspended and a volume of 25 µL was transferred in the plate containing Complete Labelling Solution. The mix was incubated for 30 minutes at room temperature, protected from light. After incubation, analysis was carried out in flow cytometry.

***Flow Cytometric Data Acquisition*:** Analysis was performed on at least 20 µL per well mixed (setting of the cytometer with 4 cycles of mixing with volumes of 40 µL), at a rate of 1 µL/sec.

***Analysis*:** Briefly, analysis was done following the global Evaluation Factor (GEF) which indicates a significant increase in mutant phenotype cell and is based on the distribution of the

negative control mutation frequency data from several proficient laboratories (Moore *et al.* 2006, Bryce *et al.* 2017).

- A test item is concluded clastogen if 2 successive doses meet or exceed the GEF for at least two out of the 2 clastogen-sensitive biomarkers,
- A test item is concluded aneugen if 2 successive doses meet or exceed the GEF for at least two out of the 2 aneugen-sensitive biomarkers,
- In case where both clastogen and aneugen-sensitive biomarkers exceeded GEF(s), the category with the greater number of significant biomarkers is selected as the predominant mode of action,
- When less than 2 clastogen- and aneugen-sensitive biomarkers meet or exceed the GEFs, the call is non-genotoxic under the test conditions used.

2.3. DCFH-DA assay

The cell model used in the assay was RAW264.7 murine macrophage cell line, provided by ATCC Cell Biology Collection (Promochem LGC). It derived from mice peritoneal macrophages transformed by the Albeson Murine Leukemia Virus. Cells were grown in 10% fetal calf serum Dulbecco's Modified Eagle Medium (DMEM, Invitrogen) supplemented with 1% penicillin-streptomycin (Sigma-Aldrich) and maintained at 37°C under a 5% carbon dioxide humidified atmosphere. It was then seeded in 96-well plates the day before exposure. Cells were then exposed to GBMs with exposure doses from 8 to 75 µg/cm² for 24 hours. ROS production was measured through OxiSelect™ Intracellular ROS Assay Kit (STA-342) as previously reported (Achawi *et al.* 2021a).

3. Results

3.1. GBMs internalization in BEAS-2B

We performed an exploratory internalization study, presented in supplementary data 2. We exposed BEAS-2B cells to RGO4 (GBM sample showing a large mean lateral size of 31.6 µm) and used optic and confocal microscopy for observation, and it seems that RGO4 can potentially be internalized in BEAS-2B cells. Although these findings are not necessarily applicable to the rest of the samples, they show that one of our largest GBM appears to be internalized in BEAS-2B cells.

3.2. DDR results

The expression of each biomarker indicating a potential aneugenic or clastogenic effect is presented in Table 2.

Six samples did not show any genotoxic effect: CB, GNP9, RGO4, RGO5, RGO7 and RGO9. Five are aneugenic only: GNP2, GNP3, GNP7, GNP8 and amorphous silica. 2 samples are aneugenic and show equivocal clastogenicity/mutagenicity (RGO3 and RGO8): indeed, they do not present two successive doses leading to a positive response for both exposure times (4h and 24h) (see section 2.2.3) but still present signs of positivity. 2 samples are both aneugenic and clastogenic: GNP1 and RGO6.

It appears that the GBMs are most likely to show aneugenic than clastogenic effects. The exposure to GBMs does not increase the p53 biomarker, except for one sample (RG08). It is worth noting that the sample that activates p53 is also aneugenic and potentially mutagenic/clastogenic.

Overall, a majority of our GNPs showed aneugenicity while a minority of them showed clastogenicity / mutagenicity.

When we obtained a positive result for genotoxicity, we usually observed a dose-dependent response.

3.3. Potential correlation between surface oxidation and genotoxicity

We tested potential correlation between physicochemical characteristics and genotoxicity impact and underscored the effect of surface oxidation. In Figure 4, we present the surface oxidation of samples grouped by their genotoxicity response (no response in green, aneugenic only in orange and both response in red), and the mean surface oxidation of their group (hatched).

GBM samples having a mean surface oxidation of 5% demonstrated no genotoxicity signal. The samples showing only an aneugenic mode of action have a 6% mean surface oxidation whereas the samples that show high genotoxicity have a 12% of mean surface oxidation, as shown in Figure 2.

It appears that the clastogenicity /mutagenicity phenomenon is rather linked to a high level of surface oxidation: this is particularly obvious for RGOs, but this observation might not be applicable to GNPs (GNP1 shows aneugenicity and mutagenicity/clastogenicity while having a low surface oxidation).

We also investigated the potential relationship between the metal contents and genotoxicity and did not observe any correlation.

3.4. ROS production and genotoxicity

We tested the relationship between the results of the genotoxicity screening test presented above and the ROS production induced by each sample (as previously assessed by the DCFH-DA assay on RAW264.7 cell model, exposed for 24 hours to the nanomaterials). The results are presented in Figure 3.

Noteworthy, despite the cell models were different (BEAS-2B for DDR assay and RAW264.7 for DCFH-DA assay), the exposure concentrations used for the two assays were consistent (*i.e.* from 8.1 µg/cm² to 75 µg/cm² for DCFH-DA assay and from 4.1 µg/cm² to 100 µg/cm² for

DDR screening assay). Please note that samples RGO3 and RGO8 were considered to be equivocal for clastogenicity / mutagenicity (see Table 2). For an easier reading of the results, we classified these two samples as positive for clastogenicity / mutagenicity in this Figure.

For ROS production, a sample was considered positive when at least two exposure concentrations led to a significant response when compared to negative control (unexposed cells). Note that all positive GBMs for ROS production led to a significant response from the lower dose (8.1 µg/cm²), except for RGO3 which led to a significant response at a moderate dose (16 µg/cm²).

It appears that some GBMs samples have the same outcome for ROS production and aneugenicity: one sample (GNP9) does not show any effect for both assays and 6 samples (GNP1, RGO3, RGO8, RGO6, GNP2, GNP3) are positive for both assays. However, 5 GBMs lead to an increased ROS production without leading to the detection of aneugenicity or clastogenicity (RGO4, RGO5, RGO7, RGO9 and CB) and 3 samples (GNP7, GNP8 and amorphous silica) are aneugenic without causing ROS production.

Clastogenicity is negative for most of our samples. However, when samples are clastogenic (4 samples: GNP1, RGO3, RGO8 and RGO6), they are also aneugenic and increase cellular ROS production. These samples have respectively a SSA of 545, 283, 270 and 440 m²/g, a lateral size of 8.4, 1.3, 32 and 1.0 µm and a surface oxidation of 11.9, 3.2, 15.9 and 17.2 %.

The only sample that does not cause ROS increase, clastogenicity and aneugenicity is GNP9. This sample, as shown in Table 2, has a low SSA (119 m²/g), a very large mean lateral size (38.6 µm) and a moderate surface oxidation (5.7 %).

4. Discussion

4.1. GBMs' genotoxicity: our results and the literature

4.1.1 In vitro studies

In this study, we tested the clastogenicity/mutagenicity and aneugenicity of 13 GBMs (including GNPs and RGOs), one carbon black and one amorphous silica on BEAS-2B cells. Carbon black is negative for both genotoxicity assays and the amorphous silica is aneugenic only. Overall, GBMs are more often aneugenic than clastogenic or mutagenic: among 13 GBMs, 8 of them are aneugenic whereas only 4 (2 of them being equivocal) are clastogenic. None of the tested samples is only clastogenic: the clastogenic samples (RGO3, RGO6, RGO8 and GNP1) are also aneugenic and cause increased ROS production. In this regard, we can probably rule out a direct clastogenicity mechanism. Some GBMs appear to have a high genotoxic impact even at quite low doses, this is not completely surprising as some of these samples also show a very high impact for other *in vitro* studies performed on RAW 264.7 (Achawi *et al.* 2021a) and on an acellular FRAS assay (Achawi *et al.* 2021b).

Carbon blacks are globally considered to be non-genotoxic (Chaudhuri *et al.* 2018). This is in agreement with our results showing no noticeable genotoxicity of our moderate specific surface area carbon black. The aneugenicity of amorphous silica has been highlighted in the work of Gonzalez *et al*. (Gonzalez *et al.* 2010, 2015) and is confirmed in our study.

Concerning GBMs, literature data tend to show mixed results: GO have mostly been considered as genotoxic (Mohamed *et al.* 2020, 2021). Their impact can be lowered with functionalization (Wang *et al.* 2013) and smallest GO tend to have more genotoxic effects (De Marzi *et al.* 2014). Another study shows that reduction enhances DNA damage caused by RGO on human retinal pigment epithelium cells (Ou *et al.* 2021). The size is also a critical parameter: the smallest RGOs are the most genotoxic whereas large ones only show a low effect (Akhavan *et al.* 2012). On BEAS-2B, GNPs also show a genotoxic impact (comet assay) even when functionalized (COOH and NH_2) (Chatterjee *et al.* 2016). Lastly, few layers graphenes (FLG) were tested on bronchial epithelial cells: the neutral and the amine-FLG cause genotoxicity whereas the carboxyl-FLG do not induce genotoxicity (Burgum, Clift, Evans, Hondow, Miller, *et al.* 2021).

Gurcan *et al*. (Gurcan *et al.* 2020) reviewed the GBM's genotoxicity modes of action: the indirect genotoxicity through the increase of ROS is particularly highlighted. To address the potential genotoxicity of GBMs, we selected few papers presenting *in vitro* investigation of GBMs' genotoxicity (presented in Table 3) (Akhavan *et al.* 2012, 2013, Li *et al.* 2014, Bengtson *et al.* 2016, Hashemi *et al.* 2016, Mittal *et al.* 2016, Arbo *et al.* 2019, Jia *et al.* 2019).

Note that methodological aspects need to be considered when comparing these results. Firstly, the tested GBMs have different physicochemical characteristics. Their exposure concentrations also vary; most papers exposed cells to several doses up to 100 µg/mL, whereas the article (Li *et al.* 2014) tested only one high exposure concentration (200 µg/mL). Moreover, the cell models differ, which can impact the measured genotoxicity. A total of 26 different GBMS were studied within these 8 studies. Tested GBMs were GOs and RGOs, functionalized in some cases with BSA and PEG and the most common investigated endpoint was the primary DNA fragmentation through the comet assay. Only 5 GBMs did not show genotoxicity while 21 of them showed moderate to strong *in vitro* genotoxicity. 13 of these samples were RGOs and among them, 8 showed potential for DNA fragmentation and the remaining 5 showed none, or only at very high dose and long exposure.

These results slightly differ from ours: we observed that most of our RGO samples do not show genotoxicity signs: neither clastogenicity / mutagenicity nor aneugenicity occurs, and only 3 of them are positive for both aneugenicity and clastogenicity. Our GNPs appear quite reactive for aneugenicity: 5 of them are positive but only one is both aneugenic and clastogenic. The comparison of the published results and ours results is delicate: our DDR testing allows specifically investigating the aneugenicity and the mutagenicity / clastogenicity mechanisms whereas DNA fragmentation highlighted with comet assay does not necessarily imply a clastogenicity: pH variation can also affect the DNA fragmentation. Moreover, comet assay does not detect aneugenicity.

4.1.2. In vivo studies

In vivo studies tend to show different results concerning GBMs genotoxicity and its potential mode of action. Weekly exposure of male mice to GO by intraperitoneal injections for up to 8 weeks resulted in DNA fragmentation in lung as well as structural chromosomal aberrations in bone marrow (El-Yamany *et al.* 2017). On the contrary, when Sprague-Dawley rats were exposed (nose-only respiratory exposure) to GNP in a 28-day study no DNA damage was found (Kim *et al.* 2016). However, in mice exposed to GO and RGO by single intratracheal instillation, an important inflammation was observed as well as DNA damage (Bengtson *et al.* 2017). Even if the authors did not make such assumptions, these results could indicate that inflammation is partially interfering with the observed DNA fragmentation. Studies using cell co-culture allowed to confirm that some GBMs could induce secondary genotoxicity through an inflammatory reaction (Burgum 2019). These studies used different rodent models and have distinct route, protocol and dose of exposure. Moreover, the GBMs tested are GO and GNP. Hence, comparing these results is delicate.

4.2. Genotoxicity and surface oxidation: a potential correlation

In Figure 2, we discussed the GBMs potential correlation between surface oxidation and genotoxicity (aneugenicity or mutagenicity/clastogenicity). It appears clearly that the negative samples for both aneugenicity and clastogenicity/mutagenicity endpoints have a low surface oxidation (mean 5 ± 1.9%) whereas samples that are clastogenic/mutagenic and aneugenic have a significantly higher surface oxidation (mean 12.1 ± 4.5 %). It hence appears that a higher surface oxidation is linked to clastogenicity/mutagenicity. This might be explained by the fact that, among other physicochemical characteristics such as size, shape or specific surface area, surface chemistry has an important impact on several genotoxicity mechanisms.

A high oxidation is not supposed to facilitate a direct interaction with DNA: the negative charge and usually higher surface defects of GOs can be a problem for a tight fixation (Liu *et al.* 2016). As an example, GO and RGO interaction with DNA was compared, with a better adsorption for RGO (Lu *et al.* 2016). Hence, even if some samples are small enough to enter the cell and even the nucleus, we cannot assume that a higher surface oxidation allows a direct contact between DNA and GBMs: the observed clastogenicity might be due to another mechanism. Oxidized surface reactivity might involve more reactive groups that could generate free radicals. It has indeed been observed previously that a modulation of surface oxidation could change the catalytic activity of graphene and graphite oxide: for producing free radicals, a sufficient oxidation is needed (Komeily-Nia *et al.* 2020).

4.3. Combining DDR testing and ROS production measurement can inform on genotoxicity mechanism

We investigated the relationship between ROS production and genotoxicity: these assays are both *in vitro* assays but were performed on different cell models: RAW264.7 cells were used for the DCFH-DA assay (ROS production) and BEAS-2B cells were used for DDR assay (clastogenicity or mutagenicity and aneugenicity). A large majority (11 out of 15) of the tested samples cause an increase of ROS production after an exposure to low to moderate doses (8 to 16 µg/cm²). A majority of the GBMs that increased ROS production also caused a positive response during genotoxicity testing, which may confirm that, for GBMs, genotoxicity is likely an indirect mechanism linked to oxidative stress. An interesting way to confirm this hypothesis would be to perform the same experiments with the adjunction of an antioxidant.

We observe that few samples increase the ROS production but do not induce genotoxicity. It might be possible that for these samples, the increased ROS production might be controlled by the cellular antioxidant defense and, under a certain threshold, will not cause indirect

genotoxicity. Similarly, the CB showed an increased ROS production, with no genotoxicity, possibly indicating that at the tested doses, the antioxidant defenses were able to avoid indirect genotoxicity.

The amorphous silica shows a different pattern: no ROS production but still an aneugenic effect. Silica's aneugenic effects has been thoroughly studied by Kirsch-Volders team, and was found to be mostly linked to chromosome migration alteration through interaction with microtubules and only minimally to the ROS production (Gonzalez *et al.* 2010). Interestingly, two GBM samples (GNP7 and GNP8) seem to show the same mechanism. For these two samples, the aneugenic impact might not be linked to oxidative stress. It is worth noting that these samples measure respectively 10.9 and 17.4 µm which probably makes these samples too large to have nuclear interaction with DNA. It might be interesting to investigate these specific GBMs' mode of action and compare it to amorphous silica's one. The other sample (GNP9) that has no impact on ROS production does not show genotoxicity either.

These results highlight that within the same family of nanomaterials, the genotoxicity mechanisms might vary. As noted previously, the genotoxicity (and its mode of action) is crucial for hazard assessment. Combining the results of genotoxicity and oxidative stress measurement can be an interesting approach to have a better insight on the genotoxicity mode of action. However, these conclusions must take into account a limitation of this study: the cell models used for each assay were different. RAW264.7 cells are murine macrophages whereas BEAS-2B cells are human epithelial respiratory cells: their cellular system might differ as well as their antioxidant capacity. Testing genotoxicity impact of GBMs in presence of antioxidant could help having a confirmation that the mechanism is oxidative stress related for some samples.

4.4. Discussing genotoxicity GBMs mechanisms

In Figure 4, we highlight the hypothetical mechanisms leading or not to *in vitro* genotoxicity among the tested GBMs.

We integrated the physicochemical characteristics possibly being involved, particularly surface oxidation (see section 4.2) and the information concerning ROS production caused by GBMs. We can spot five groups of materials that appear to have different outcomes for genotoxicity and various modes of action:

1. No detectable genotoxicity or ROS production (GNP9): this sample induces neither increase in ROS production nor genotoxicity. The very large lateral size (38.6 µm) may prevent this substance from penetrating the cells combined with the low surface oxidation of this sample (5.7%) which might not cause the production of free radicals.
2. Increased ROS production as well as aneugenicity and clastogenicity/mutagenicity (RGO3, RGO8, and RGO6): the high surface oxidation of these samples might increase the presence of oxygen chemical groups on their surface, leading to a free radical's release which could eventually cause overwhelming ROS production and/or interaction with DNA.
3. Aneugenicity and no detected ROS production or mutagenicity/clastogenicity (GNP7, GNP8, silica): for this group, we can suppose that the mode of action does not involve oxidative stress but disturbance of mitotic apparatus (*e.g.*, chromosome migration alteration during mitosis).
4. Increased ROS production, aneugenicity (GNP2, GNP3) and clastogenicity (GNP1): these samples show very small lateral size (approximately 1 µm or less) compared to the rest of the pool, which could allow the samples to directly interact with DNA.
5. Increased ROS production without any genotoxic effect (RGO5, RGO4, RGO7, RGO9, CB): these samples show an increase of ROS production which, at the tested exposure

doses, might be controlled by the cell antioxidant defenses and will not cause genotoxicity.

5. Conclusion

This work allows having a better insight of the potential genotoxicity of GBMs and underlines that within the same family of nanomaterials (GBMs) and among only two subfamilies (GNPs and RGOs), we can still observe different outcomes and potential genotoxicity mechanisms. We can conclude that most of the tested samples appear to induce an indirect, oxidative stress-driven genotoxicity. Using only two *in vitro* assays (HTS assay for genotoxicity and DCFH-DA assay for ROS production), combined with a relevant physicochemical characterization, we were able to formulate several hypotheses that shall be explored in the future in order to have a clearer insight of potential GBMs genotoxicity mechanisms. For a screening step and/or grouping purposes, this combination of DDR and DCFH-DA assays appears relevant and adapted to 2D carbonaceous materials such as graphene-based materials.

Considering the increasing demand for nanomaterials-based innovation and the necessity to test every nanoform of each nanomaterial, a systematic case-by-case approach appears impossible for toxicity study. Yet, the hazard assessment is a non-negotiable step for the entry in any market and an inescapable stage of research and development in industry. High throughput screening present undisputable advantages: it is quick, often standardized, and cheapest than considering a complete study of each nanomaterial and can allow to rank materials of interest before going any further in the development process. The approach proposed in this paper allows to have an insight on GBM's potential structure-activity relationship involved in genotoxicity and to have a clearer understanding of their mode of action. These indications can represent one more step toward safe-by-design GBMs.

Funding

This work was supported by Michelin.

Declaration of interest

Salma Achawi and Bruno Feneon are employees of Michelin company, a global tire and rubber goods manufacturer.

References

Achawi, S., Feneon, B., Pourchez, J., and Forest, V., 2021a. Structure-Activity Relationship of Graphene-Based Materials: Impact of the Surface Chemistry, Surface Specific Area and Lateral Size on Their In Vitro Toxicity. *Nanomaterials (Basel, Switzerland)*, 11 (11), 2963.

Achawi, S., Feneon, B., Pourchez, J., and Forest, V., 2021b. Assessing biological oxidative damage induced by graphene-based materials: An asset for grouping approaches using the FRAS assay. *Regulatory toxicology and pharmacology: RTP*, 127, 105067.

Ain, Q.T., Haq, S.H., Alshammari, A., Al-Mutlaq, M.A., and Anjum, M.N., 2019. The systemic effect of PEG-nGO-induced oxidative stress in vivo in a rodent model. *Beilstein Journal of Nanotechnology*, 10, 901–911.

Åkerlund, E., Islam, M.S., McCarrick, S., Alfaro-Moreno, E., and Karlsson, H.L., 2019. Inflammation and (secondary) genotoxicity of Ni and NiO nanoparticles. *Nanotoxicology*, 13 (8), 1060–1072.

Akhavan, O., Ghaderi, E., and Akhavan, A., 2012. Size-dependent genotoxicity of graphene nanoplatelets in human stem cells. *Biomaterials*, 33 (32), 8017–8025.

Akhavan, O., Ghaderi, E., Emamy, H., and Akhavan, F., 2013. Genotoxicity of graphene nanoribbons in human mesenchymal stem cells. *Carbon*, 54, 419–431.

Arbo, M.D., Altknecht, L.F., Cattani, S., Braga, W.V., Peruzzi, C.P., Cestonaro, L.V., Göethel, G., Durán, N., and Garcia, S.C., 2019. In vitro cardiotoxicity evaluation of graphene oxide. *Mutation Research. Genetic Toxicology and Environmental Mutagenesis*, 841, 8–13.

Bengtson, S., Kling, K., Madsen, A.M., Noergaard, A.W., Jacobsen, N.R., Clausen, P.A., Alonso, B., Pesquera, A., Zurutuza, A., Ramos, R., Okuno, H., Dijon, J., Wallin, H., and Vogel, U., 2016. No cytotoxicity or genotoxicity of graphene and graphene oxide in murine lung epithelial FE1 cells in vitro. *Environmental and Molecular Mutagenesis*, 57 (6), 469–482.

Bengtson, S., Knudsen, K.B., Kyjovska, Z.O., Berthing, T., Skaug, V., Levin, M., Koponen, I.K., Shivayogimath, A., Booth, T.J., Alonso, B., Pesquera, A., Zurutuza, A., Thomsen, B.L., Troelsen, J.T., Jacobsen, N.R., and Vogel, U., 2017. Differences in inflammation and acute phase response but similar genotoxicity in mice following pulmonary exposure to graphene oxide and reduced graphene oxide. *PloS One*, 12 (6), e0178355.

Bhaskaran, A., May, D., Rand-Weaver, M., and Tyler, C.R., 1999. Fish p53 as a possible biomarker for genotoxins in the aquatic environment. *Environmental and Molecular Mutagenesis*, 33 (3), 177–184.

Bignold, L.P., 2009. Mechanisms of clastogen-induced chromosomal aberrations: a critical review and description of a model based on failures of tethering of DNA strand ends to strand-breaking enzymes. *Mutation Research*, 681 (2–3), 271–298.

Bonner, W.M., Redon, C.E., Dickey, J.S., Nakamura, A.J., Sedelnikova, O.A., Solier, S., and Pommier, Y., 2008. GammaH2AX and cancer. *Nature Reviews. Cancer*, 8 (12), 957–967.

Bryce, S.M., Bernacki, D.T., Bemis, J.C., Spellman, R.A., Engel, M.E., Schuler, M., Lorge, E., Heikkinen, P.T., Hemmann, U., Thybaud, V., Wilde, S., Queisser, N., Sutter, A., Zeller,

A., Guérard, M., Kirkland, D., and Dertinger, S.D., 2017. Interlaboratory evaluation of a multiplexed high information content in vitro genotoxicity assay. *Environmental and Molecular Mutagenesis*, 58 (3), 146–161.

Burgum, M., 2019. In Vitro Lung Models to Assess the Mechanistic Genotoxicity of Characterised Few-Layer Graphene. Swansea University.

Burgum, M., Clift, M., Evans, S.J., Hondow, N., Miller, M., Lopez, S.B., Williams, A., Tarat, A., Jenkins, G.J., and Doak, S.H., 2021. In Vitro Primary-Indirect Genotoxicity in Bronchial Epithelial Cells Promoted by Industrially Relevant Few-Layer Graphene. *Small*, 17 (15), 2002551.

Burgum, M.J., Clift, M.J.D., Evans, S.J., Hondow, N., Tarat, A., Jenkins, G.J., and Doak, S.H., 2021. Few-layer graphene induces both primary and secondary genotoxicity in epithelial barrier models in vitro. *Journal of Nanobiotechnology*, 19 (1), 24.

Chatterjee, N., Yang, J., and Choi, J., 2016. Differential genotoxic and epigenotoxic effects of graphene family nanomaterials (GFNs) in human bronchial epithelial cells. *Mutation Research. Genetic Toxicology and Environmental Mutagenesis*, 798–799, 1–10.

Chaudhuri, I., Fruijtier-Pölloth, C., Ngiewih, Y., and Levy, L., 2018. Evaluating the evidence on genotoxicity and reproductive toxicity of carbon black: a critical review. *Critical Reviews in Toxicology*, 48 (2), 143–169.

Chen, M., Yin, J., Liang, Y., Yuan, S., Wang, F., Song, M., and Wang, H., 2016. Oxidative stress and immunotoxicity induced by graphene oxide in zebrafish. *Aquatic Toxicology (Amsterdam, Netherlands)*, 174, 54–60.

Corvi, R. and Madia, F., 2017. In vitro genotoxicity testing-Can the performance be enhanced? *Food and Chemical Toxicology: An International Journal Published for the British Industrial Biological Research Association*, 106 (Pt B), 600–608.

De Marzi, L., Ottaviano, L., Perrozzi, F., Nardone, M., Santucci, S., De Lapuente, J., Borras, M., Treossi, E., Palermo, V., and Poma, A., 2014. Flake size-dependent cyto and genotoxic evaluation of graphene oxide on in vitro A549, CaCo2 and vero cell lines. *Journal of Biological Regulators and Homeostatic Agents*, 28 (2), 281–289.

DeMarini, D.M., 2019. The role of genotoxicity in carcinogenesis. *In*: R.A. Baan, B.W. Stewart, and K. Straif, eds. *Tumour Site Concordance and Mechanisms of Carcinogenesis*. Lyon (FR): International Agency for Research on Cancer.

Deng, S., Fu, A., Junaid, M., Wang, Y., Yin, Q., Fu, C., Liu, L., Su, D.-S., Bian, W.-P., and Pei, D.-S., 2019. Nitrogen-doped graphene quantum dots (N-GQDs) perturb redox-sensitive system via the selective inhibition of antioxidant enzyme activities in zebrafish. *Biomaterials*, 206, 61–72.

Di Cristo, L., Grimaldi, B., Catelani, T., Vázquez, E., Pompa, P.P., and Sabella, S., 2020. Repeated exposure to aerosolized graphene oxide mediates autophagy inhibition and inflammation in a three-dimensional human airway model. *Materials Today. Bio*, 6, 100050.

Dizdaroglu, M., Jaruga, P., Birincioglu, M., and Rodriguez, H., 2002. Free radical-induced damage to DNA: mechanisms and measurement. *Free Radical Biology & Medicine*, 32 (11), 1102–1115.

Doak, S.H., Manshian, B., Jenkins, G.J.S., and Singh, N., 2012. In vitro genotoxicity testing strategy for nanomaterials and the adaptation of current OECD guidelines. *Mutation Research*, 745 (1–2), 104–111.

Dziewięcka, M., Karpeta-Kaczmarek, J., Augustyniak, M., and Rost-Roszkowska, M., 2017. Short-term in vivo exposure to graphene oxide can cause damage to the gut and testis. *Journal of Hazardous Materials*, 328, 80–89.

El-Yamany, N.A., Mohamed, F.F., Salaheldin, T.A., Tohamy, A.A., Abd El-Mohsen, W.N., and Amin, A.S., 2017. Graphene oxide nanosheets induced genotoxicity and pulmonary injury in mice. *Experimental and Toxicologic Pathology: Official Journal of the Gesellschaft Fur Toxikologische Pathologie*, 69 (6), 383–392.

Evans, S.J., Clift, M.J.D., Singh, N., de Oliveira Mallia, J., Burgum, M., Wills, J.W., Wilkinson, T.S., Jenkins, G.J.S., and Doak, S.H., 2017. Critical review of the current and future challenges associated with advanced in vitro systems towards the study of nanoparticle (secondary) genotoxicity. *Mutagenesis*, 32 (1), 233–241.

Fadeel, B., Bussy, C., Merino, S., Vázquez, E., Flahaut, E., Mouchet, F., Evariste, L., Gauthier, L., Koivisto, A.J., Vogel, U., Martín, C., Delogu, L.G., Buerki-Thurnherr, T., Wick, P., Beloin-Saint-Pierre, D., Hischier, R., Pelin, M., Candotto Carniel, F., Tretiach, M., Cesca, F., Benfenati, F., Scaini, D., Ballerini, L., Kostarelos, K., Prato, M., and Bianco, A., 2018. Safety Assessment of Graphene-Based Materials: Focus on Human Health and the Environment. *ACS nano*, 12 (11), 10582–10620.

Gonzalez, L., De Santis Puzzonia, M., Ricci, R., Aureli, F., Guarguaglini, G., Cubadda, F., Leyns, L., Cundari, E., and Kirsch-Volders, M., 2015. Amorphous silica nanoparticles alter microtubule dynamics and cell migration. *Nanotoxicology*, 9 (6), 729–736.

Gonzalez, L., Decordier, I., and Kirsch-Volders, M., 2010. Induction of chromosome malsegregation by nanomaterials. *Biochemical Society Transactions*, 38 (6), 1691–1697.

Gonzalez, L., Sanderson, B.J.S., and Kirsch-Volders, M., 2011. Adaptations of the in vitro MN assay for the genotoxicity assessment of nanomaterials. *Mutagenesis*, 26 (1), 185–191.

Gurcan, C., Taheri, H., Bianco, A., Delogu, L.G., and Yilmazer, A., 2020. A closer look at the genotoxicity of graphene based materials. *Journal of Physics: Materials*, 3 (1), 014007.

Gurunathan, S., Kang, M.-H., Jeyaraj, M., and Kim, J.-H., 2019a. Differential Immunomodulatory Effect of Graphene Oxide and Vanillin-Functionalized Graphene Oxide Nanoparticles in Human Acute Monocytic Leukemia Cell Line (THP-1). *International Journal of Molecular Sciences*, 20 (2), E247.

Gurunathan, S., Kang, M.-H., Jeyaraj, M., and Kim, J.-H., 2019b. Differential Cytotoxicity of Different Sizes of Graphene Oxide Nanoparticles in Leydig (TM3) and Sertoli (TM4) Cells. *Nanomaterials (Basel, Switzerland)*, 9 (2), E139.

Hamilton, M.E., Bols, N.C., and Duncker, B.P., 2018. The characterization of γH2AX and p53 as biomarkers of genotoxic stress in a rainbow trout (Oncorhynchus mykiss) brain cell line. *Chemosphere*, 201, 850–858.

Hashemi, E., Akhavan, O., Shamsara, M., Daliri, M., Dashtizad, M., and Farmany, A., 2016. Synthesis and cyto-genotoxicity evaluation of graphene on mice spermatogonial stem cells. *Colloids and Surfaces. B, Biointerfaces*, 146, 770–776.

Hayashi, Y., 1992. Overview of genotoxic carcinogens and non-genotoxic carcinogens. *Experimental and Toxicologic Pathology: Official Journal of the Gesellschaft Fur Toxikologische Pathologie*, 44 (8), 465–471.

Hayman, L., Chaudhry, W.R., Revin, V.V., Zhelev, N., and Bourdon, J.-C., 2019. What is the potential of p53 isoforms as a predictive biomarker in the treatment of cancer? *Expert Review of Molecular Diagnostics*, 19 (2), 149–159.

Inshakova, E. and Inshakov, O., 2017. World market for nanomaterials: structure and trends. *MATEC Web of Conferences*, 129, 02013.

Jarosz, A., Skoda, M., Dudek, I., and Szukiewicz, D., 2016. Oxidative Stress and Mitochondrial Activation as the Main Mechanisms Underlying Graphene Toxicity against Human Cancer Cells. *Oxidative Medicine and Cellular Longevity*, 2016, 5851035.

Jaworski, S., Strojny, B., Sawosz, E., Wierzbicki, M., Grodzik, M., Kutwin, M., Daniluk, K., and Chwalibog, A., 2019. Degradation of Mitochondria and Oxidative Stress as the Main Mechanism of Toxicity of Pristine Graphene on U87 Glioblastoma Cells and Tumors and HS-5 Cells. *International Journal of Molecular Sciences*, 20 (3), E650.

Jenkins, G.J.S., Zaïr, Z., Johnson, G.E., and Doak, S.H., 2010. Genotoxic thresholds, DNA repair, and susceptibility in human populations. *Toxicology*, 278 (3), 305–310.

Jia, P.-P., Sun, T., Junaid, M., Yang, L., Ma, Y.-B., Cui, Z.-S., Wei, D.-P., Shi, H.-F., and Pei, D.-S., 2019. Nanotoxicity of different sizes of graphene (G) and graphene oxide (GO) in vitro and in vivo. *Environmental Pollution (Barking, Essex: 1987)*, 247, 595–606.

Khoury, L., Zalko, D., and Audebert, M., 2016. Complementarity of phosphorylated histones H2AX and H3 quantification in different cell lines for genotoxicity screening. *Archives of Toxicology*, 90 (8), 1983–1995.

Kim, J.K., Shin, J.H., Lee, J.S., Hwang, J.H., Lee, J.H., Baek, J.E., Kim, T.G., Kim, B.W., Kim, J.S., Lee, G.H., Ahn, K., Han, S.G., Bello, D., and Yu, I.J., 2016. 28-Day inhalation toxicity of graphene nanoplatelets in Sprague-Dawley rats. *Nanotoxicology*, 10 (7), 891–901.

Kinner, A., Wu, W., Staudt, C., and Iliakis, G., 2008. Gamma-H2AX in recognition and signaling of DNA double-strand breaks in the context of chromatin. *Nucleic Acids Research*, 36 (17), 5678–5694.

Kirsch-Volders, M., Vanhauwaert, A., Eichenlaub-Ritter, U., and Decordier, I., 2003. Indirect mechanisms of genotoxicity. *Toxicology Letters*, 140–141, 63–74.

Komeily-Nia, Z., Chen, J.-Y., Nasri-Nasrabadi, B., Lei, W.-W., Yuan, B., Zhang, J., Qu, L.-T., Gupta, A., and Li, J.-L., 2020. The key structural features governing the free radicals and catalytic activity of graphite/graphene oxide. *Physical chemistry chemical physics: PCCP*, 22 (5), 3112–3121.

Kopp, B., Khoury, L., and Audebert, M., 2019. Validation of the γH2AX biomarker for genotoxicity assessment: a review. *Archives of Toxicology*, 93 (8), 2103–2114.

Kumar, A., Dobrovolsky, V.N., Dhawan, A., and Shanker, R., eds., 2018. Mutagenicity: Assays and Applications. *In*: *Mutagenicity: Assays and Applications*. Academic Press, iii.

Li, Y., Feng, L., Shi, X., Wang, X., Yang, Y., Yang, K., Liu, T., Yang, G., and Liu, Z., 2014. Surface coating-dependent cytotoxicity and degradation of graphene derivatives: towards the design of non-toxic, degradable nano-graphene. *Small (Weinheim an Der Bergstrasse, Germany)*, 10 (8), 1544–1554.

Liu, B., Salgado, S., Maheshwari, V., and Liu, J., 2016. DNA adsorbed on graphene and graphene oxide: Fundamental interactions, desorption and applications. *Current Opinion in Colloid & Interface Science*, 26, 41–49.

Liu, Y., Luo, Y., Wu, J., Wang, Y., Yang, X., Yang, R., Wang, B., Yang, J., and Zhang, N., 2013. Graphene oxide can induce in vitro and in vivo mutagenesis. *Scientific Reports*, 3, 3469.

Lu, C., Huang, P.-J.J., Liu, B., Ying, Y., and Liu, J., 2016. Comparison of Graphene Oxide and Reduced Graphene Oxide for DNA Adsorption and Sensing. *Langmuir*, 32 (41), 10776–10783.

Magdolenova, Z., Collins, A., Kumar, A., Dhawan, A., Stone, V., and Dusinska, M., 2014. Mechanisms of genotoxicity. A review of in vitro and in vivo studies with engineered nanoparticles. *Nanotoxicology*, 8 (3), 233–278.

Matsuzaki, K., Harada, A., Takeiri, A., Tanaka, K., and Mishima, M., 2010. Whole cell-ELISA to measure the gammaH2AX response of six aneugens and eight DNA-damaging chemicals. *Mutation Research*, 700 (1–2), 71–79.

Mishima, M., 2017. Chromosomal aberrations, clastogens vs aneugens. *Frontiers in Bioscience (Scholar Edition)*, 9, 1–16.

Mittal, S., Kumar, V., Dhiman, N., Chauhan, L.K.S., Pasricha, R., and Pandey, A.K., 2016. Physico-chemical properties based differential toxicity of graphene oxide/reduced graphene oxide in human lung cells mediated through oxidative stress. *Scientific Reports*, 6, 39548.

Mohamed, H.R.H., Welson, M., Yaseen, A.E., and El-Ghor, A., 2021. Induction of chromosomal and DNA damage and histological alterations by graphene oxide nanoparticles in Swiss mice. *Drug and Chemical Toxicology*, 44 (6), 631–641.

Mohamed, H.R.H., Welson, M., Yaseen, A.E., and El-Ghor, A.A., 2020. Estimation of genomic instability and mutation induction by graphene oxide nanoparticles in mice liver and brain tissues. *Environmental Science and Pollution Research International*, 27 (1), 264–278.

Moore, M.M., Honma, M., Clements, J., Bolcsfoldi, G., Burlinson, B., Cifone, M., Clarke, J., Delongchamp, R., Durward, R., Fellows, M., Gollapudi, B., Hou, S., Jenkinson, P., Lloyd, M., Majeska, J., Myhr, B., O'Donovan, M., Omori, T., Riach, C., San, R., Stankowski, L.F., Thakur, A.K., Van Goethem, F., Wakuri, S., and Yoshimura, I., 2006. Mouse lymphoma thymidine kinase gene mutation assay: follow-up meeting of the International Workshop on Genotoxicity Testing--Aberdeen, Scotland, 2003--Assay acceptance criteria, positive controls, and data evaluation. *Environmental and Molecular Mutagenesis*, 47 (1), 1–5.

More, S.J., Bampidis, V., Bragard, C., Halldorsson, T.I., Hernández-Jerez, A.F., Hougaard Bennekou, S., Koutsoumanis, K., Lambré, C., Machera, K., Naegeli, H., Nielsen, S.S., Schlatter, J., Schrenk, D., Turck, D., Younes, M., Aquilina, G., Bignami, M., Bolognesi, C., Crebelli, R., Gürtler, R., Marcon, F., Nielsen, E., Vleminckx, C., Carfì, M., Martino, C., Maurici, D., Parra Morte, J., Rossi, A., and Benford, D., 2021. Guidance on aneugenicity assessment. *EFSA Journal*, 19 (8), e06770.

Novoselov, K.S., Geim, A.K., Morozov, S.V., Jiang, D., Zhang, Y., Dubonos, S.V., Grigorieva, I.V., and Firsov, A.A., 2004. Electric field effect in atomically thin carbon films. *Science (New York, N.Y.)*, 306 (5696), 666–669.

OECD, 2016. *Test No. 487: In Vitro Mammalian Cell Micronucleus Test*. Paris: Organisation for Economic Co-operation and Development.

Ou, L., Lv, X., Wu, Z., Xia, W., Huang, Y., Chen, L., Sun, W., Qi, Y., Yang, M., and Qi, L., 2021. Oxygen content-related DNA damage of graphene oxide on human retinal pigment epithelium cells. *Journal of Materials Science. Materials in Medicine*, 32 (2), 20.

Parry, E.M., Parry, J.M., Corso, C., Doherty, A., Haddad, F., Hermine, T.F., Johnson, G., Kayani, M., Quick, E., Warr, T., and Williamson, J., 2002. Detection and characterization of mechanisms of action of aneugenic chemicals. *Mutagenesis*, 17 (6), 509–521.

Parry, J.M., Parry, E.M., Bourner, R., Doherty, A., Ellard, S., O'Donovan, J., Hoebee, B., de Stoppelaar, J.M., Mohn, G.R., Onfelt, A., Renglin, A., Schultz, N., Söderpalm-Berndes, C., Jensen, K.G., Kirsch-Volders, M., Elhajouji, A., Van Hummelen, P., Degrassi, F., Antoccia, A., Cimini, D., Izzo, M., Tanzarella, C., Adler, I.D., Kliesch, U., and Hess, P., 1996. The detection and evaluation of aneugenic chemicals. *Mutation Research*, 353 (1–2), 11–46.

Phillips, D.H. and Arlt, V.M., 2009. Genotoxicity: damage to DNA and its consequences. *EXS*, 99, 87–110.

Pieper, H., Chercheja, S., Eigler, S., Halbig, C.E., Filipovic, M.R., and Mokhir, A., 2016. Endoperoxides Revealed as Origin of the Toxicity of Graphene Oxide. *Angewandte Chemie (International Ed. in English)*, 55 (1), 405–407.

Ren, H., Wang, C., Zhang, J., Zhou, X., Xu, D., Zheng, J., Guo, S., and Zhang, J., 2010. DNA cleavage system of nanosized graphene oxide sheets and copper ions. *ACS nano*, 4 (12), 7169–7174.

Rogakou, E.P., Pilch, D.R., Orr, A.H., Ivanova, V.S., and Bonner, W.M., 1998. DNA double-stranded breaks induce histone H2AX phosphorylation on serine 139. *The Journal of Biological Chemistry*, 273 (10), 5858–5868.

Schwarz-Plaschg, C., Kallhoff, A., and Eisenberger, I., 2017. Making Nanomaterials Safer by Design? *NanoEthics*, 11 (3), 277–281.

Stead, A.G., Hasselblad, V., Creason, J.P., and Claxton, L., 1981. Modeling the Ames test. *Mutation Research/Environmental Mutagenesis and Related Subjects*, 85 (1), 13–27.

Sukumaran, S.K., Ranganatha, R., and Chakravarthy, S., 2016. High-throughput approaches for genotoxicity testing in drug development: recent advances. *International Journal of High Throughput Screening*, 1.

Sun, Y., Dai, H., Chen, S., Xu, M., Wang, X., Zhang, Y., Xu, S., Xu, A., Weng, J., Liu, S., and Wu, L., 2018. Graphene oxide regulates cox2 in human embryonic kidney 293T cells via epigenetic mechanisms: dynamic chromosomal interactions. *Nanotoxicology*, 12 (2), 117–137.

Tabish, T.A., Zhang, S., and Winyard, P.G., 2018. Developing the next generation of graphene-based platforms for cancer therapeutics: The potential role of reactive oxygen species. *Redox Biology*, 15, 34–40.

Vranic, S., Rodrigues, A.F., Buggio, M., Newman, L., White, M.R.H., Spiller, D.G., Bussy, C., and Kostarelos, K., 2018. Live Imaging of Label-Free Graphene Oxide Reveals Critical Factors Causing Oxidative-Stress-Mediated Cellular Responses. *ACS nano*, 12 (2), 1373–1389.

Wang, A., Pu, K., Dong, B., Liu, Y., Zhang, L., Zhang, Z., Duan, W., and Zhu, Y., 2013. Role of surface charge and oxidative stress in cytotoxicity and genotoxicity of graphene oxide towards human lung fibroblast cells. *Journal of applied toxicology: JAT*, 33 (10), 1156–1164.

Wang, K., Ruan, J., Song, H., Zhang, J., Wo, Y., Guo, S., and Cui, D., 2010. Biocompatibility of Graphene Oxide. *Nanoscale Res Lett*, 6 (1), 8.

Wilde, S., Queisser, N., and Sutter, A., 2020. Image analysis of mechanistic protein biomarkers for the characterization of genotoxicants: Aneugens, clastogens, and reactive oxygen species inducers. *Environmental and Molecular Mutagenesis*, 61 (5), 534–550.

Table 1 – Physicochemical features of the tested nanomaterials. BET: Brunauer, Emmett and Teller, EM: Electron Microscopy, XPS: X-ray spectroscopy.

	Specific surface area, m^2/g (BET)	Mean lateral Size in µm (EM)	Surface oxidation atomic % (XPS)
GNP1	283	1.3	3.2
GNP2	439	0.7	6.3
GNP3	692	0.5	7.6
GNP7	89	10.9	4.2
GNP8	168	17.3	5.9
GNP9	119	38.6	5.7
rGO3	545	8.3	11.9
rGO4	880	31.6	7.2
rGO5	830	7.0	2.7
rGO6	270	32.0	15.9
rGO7	810	15.1	6.7
rGO8	440	1.0	17.2
rGO9	870	1.1	2.6
CB	112	0.4	2.6
Amorphous Silica	160	0.1	70.0

Table 2 - DDR results.

	Aneugenic		Clastogenic / Mutagenic		P53 activation
	4h	24h	4h	24h	total
CB	negative	negative	negative	negative	negative
Amorphous silica	**50**	**75**	**75**	negative	negative
GNP1	**38**	**50**	**50**	**50**	negative
GNP2	**38**	**25**	**50**	negative	negative
GNP3	**8**	**4**	**75**	negative	negative
GNP7	**4**	**75**	negative	negative	negative
GNP8	**38**	**50**	negative	negative	negative
GNP9	**38**	negative	negative	negative	negative
RGO3	**75**	**50**	**50**	**100**	negative
RGO4	**100**	**100**	negative	negative	negative
RGO6	**50**	**17**	25	50	negative
RGO5	negative	negative	negative	negative	negative
RGO7	negative	negative	**100**	negative	negative
RGO8	**17**	**17**	**25**	**100**	positive
RGO9	negative	negative	negative	negative	negative

negative : no response detected

number : concentration (in µg/cm²) for which we noted a significant response

Positive

Equivocal

Negative

Table 3 - Presentation of papers studying GBMs' genotoxicity. Studies colored in green: did not show genotoxicity, in yellow: showed mixed result, in red: showed genotoxicity. GO: Graphene Oxide, RGO: Reduced graphene oxide, S: Significant, NS: Non-significant.

First Author	Year	Number of GBM	GBM type	Physicochemical characteristics	Exposure time	Dose (µg/mL)	Model	Assay	Conclusions	Note
Akhavan O	2012	4	RGO	Lateral Size : 11-3100 nm Thickness : 0.7-2.3nm Oxidation : 30-50%	1h	0.01-100	hMSCs	Comet assay Chromosomal aberration	S from dose 0.1 to 100 µg/mL S from dose 0.1 for some, some NS.	Obvious genotoxicity. The largest RGOs are less genotoxic
Arbo MD	2019	1	GO	Lateral Size : ~550 nm Thickness : ~1nm	24h	10-100	H9c2	Comet assay Low molecular Weigh DNA fraction	S from dose 40 µg/mL	GO show moderate genotoxicity
Bengtson S	2016	3	GO RGO	Size dispersion : 157-335 (DLS) Oxidation : 8-27%	24h	50-200	FE1	Comet assay	NS for all doses	No genotoxicity demonstrated.
Jia PP	2019	6	G GO	Lateral Size : 29-1000 nm Thickness : 1nm Oxidation : 5-33%	24h	5-100	HEK 293T	Comet assay	S from dose 5 to 25µg/mL	Only the largest, less oxidized G show genotoxicity at higher doses
Li Y	2013	5	GO GO PEG GO BSA RGO PEG RGO BSA	Lateral Size : 30-450 nm Thickness : 1-15 nm	24h 48h 72h	200	U937	Comet assay	S at 24h for only GO S at 48h,for GO and RGO BSA S at 72h, for GO, RGO BSA, RGO PEG and GO BSA	A very high dose and long exposure are necessary to observe genotoxicity
Mittal S	2016	3	GO, RGO	Lateral Size : 90-750 nm	3h 6h	1-100	BEAS-2B A549	Micronucleus	S for dose 25 (3h) and 10 µg/mL(6h) for GO S from dose 1µg/mL for one RGO S at dose 100µg/mL (6h) for other RGO	Strong genotoxicity for 2 GBMs, none for one of them. The genotoxicity is lower when tested on A459
Hashemi E	2016	2	GO RGO	Thickness : 0.8 nm	24h	0.1-400	SSCs	Comet	S from dose 10µg/mL (GO) and increased (no significativity found?) from dose 100µg/mL (RGO)	Strong genotoxicity for GO, moderate for RGO
Akhavan O	2012	2	RGOSs RGONRs	Lateral Size : 11-3100 nm Thickness : 1 nm Oxidation : 30-50%	1 5 24 96	0.01-100	hMSCs	Comet assay Chromosomal aberration RNA efflux	RNA efflux : S at dose 100µg/mL and 24h (RGOS) and S at dose 100µg/mL and 1h (RGONR). Chromosomal abberation/Comet : S from dose 1µg/mL at 1 h exposure (RGONR tested only)	Strong genotoxicity for RGONR (from lower dose and exposure time)

Figure 1

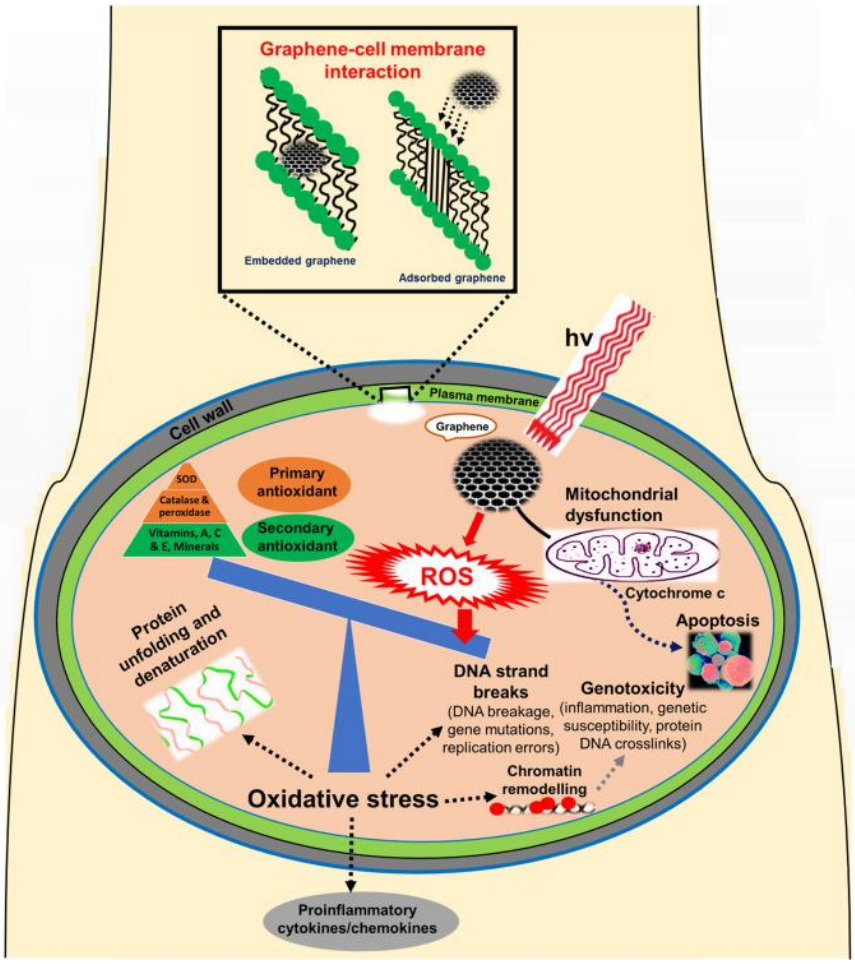
Graphene-cell membrane interaction
Embedded graphene
Adsorbed graphene
hv
Plasma membrane
Cell wall
Graphene
SOD
Catalase & peroxidase
Vitamins, A, C & E, Minerals
Primary antioxidant
Secondary antioxidant
ROS
Mitochondrial dysfunction
Cytochrome c
Apoptosis
Protein unfolding and denaturation
DNA strand breaks
(DNA breakage, gene mutations, replication errors)
Genotoxicity
(inflammation, genetic susceptibility, protein DNA crosslinks)
Chromatin remodelling
Oxidative stress
Proinflammatory cytokines/chemokines

Figure 2

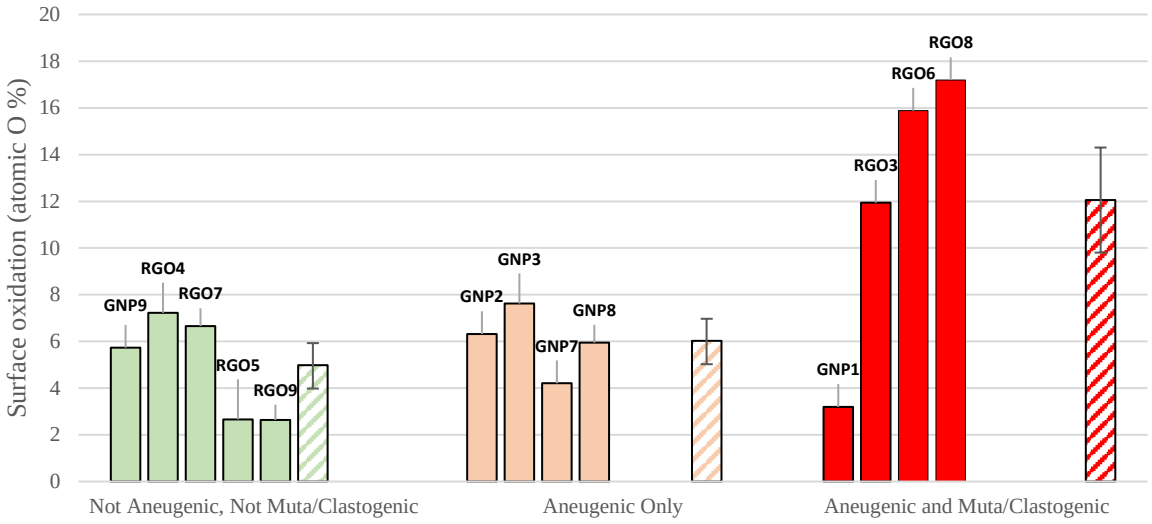
Surface oxidation (atomic O %)
20
18
16
14
12
10
8
6
4
2
0
GNP9
RGO4
RGO7
RGO5
RGO9
GNP2
GNP3
GNP7
GNP8
GNP1
RGO3
RGO6
RGO8
Not Aneugenic, Not Muta/Clastogenic
Aneugenic Only
Aneugenic and Muta/Clastogenic

Figure 3

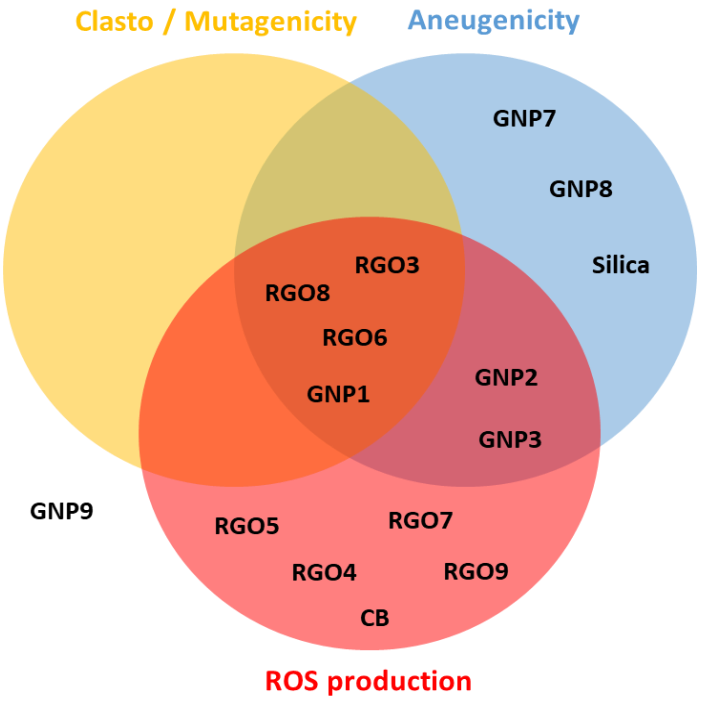
Clasto / Mutagenicity
Aneugenicity
GNP7
GNP8
Silica
RGO3
RGO8
RGO6
GNP2
GNP1
GNP3
GNP9
RGO5
RGO7
RGO4
RGO9
CB
ROS production

Figure 4

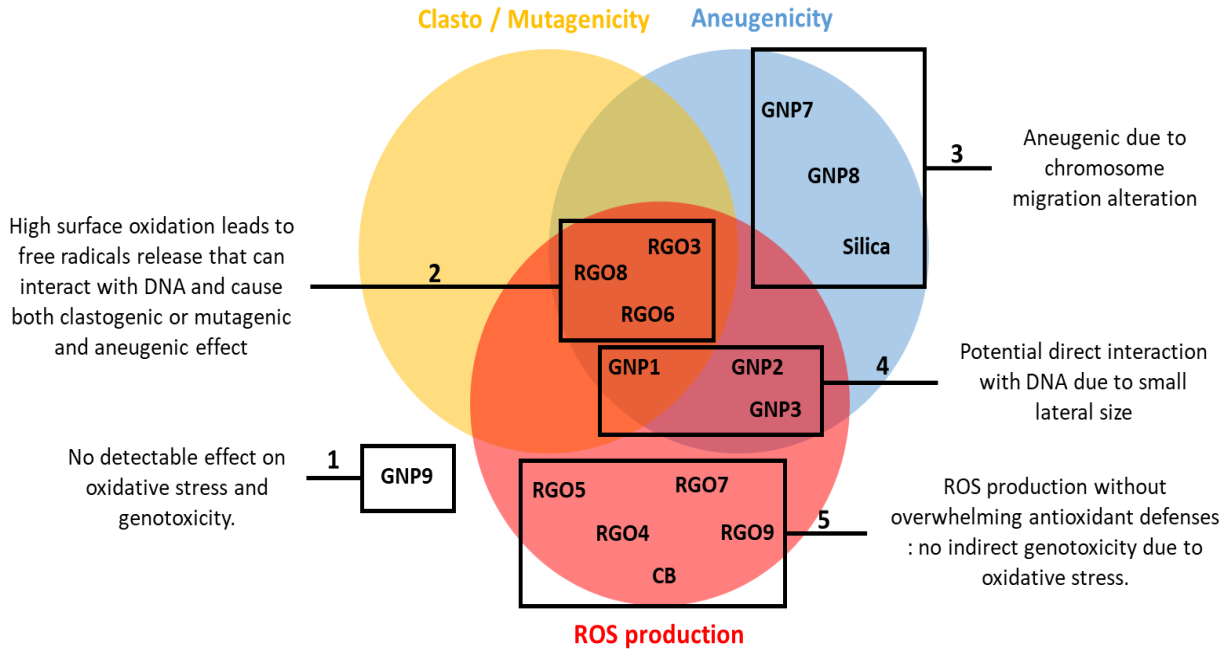
Clasto / Mutagenicity
Aneugenicity
GNP7
GNP8
Silica
3
Aneugenic due to chromosome migration alteration
High surface oxidation leads to free radicals release that can interact with DNA and cause both clastogenic or mutagenic and aneugenic effect
2
RGO3
RGO8
RGO6
GNP1
GNP2
GNP3
4
Potential direct interaction with DNA due to small lateral size
No detectable effect on oxidative stress and genotoxicity.
1
GNP9
RGO5
RGO7
RGO4
RGO9
CB
5
ROS production without overwhelming antioxidant defenses : no indirect genotoxicity due to oxidative stress.
ROS production

Figure captions

Figure 1 - Oxidative stress generated by GBMs can lead to genotoxicity. From [22], reproduced with permission.

Figure 2 - Surface oxidation depending on the genotoxicity results.

Figure 3 - Genotoxicity mode of action and ROS production.

Figure 4 - Hypothetical genotoxicity mode of action of the tested GBMs.

Supplementary data

Supplementary data 1: Physicochemical characterization

ICP Analysis

	ICP results (ppm)																						
	Al	B	Ba	Ca	Co	Cr	Cu	Fe	K	Li	Mg	Mn	Mo	Na	Ni	S	Si	Sn	Sr	Ti	V	Zn	Zr
GNP1	54	16	1	90	0	2	2	21	47	0	45	0	7	40	0	44	0	4	0	20	4	32	13
GNP2	430	92	3	538	0	1	5	1008	201	0	304	13	2	162	5	136	0	368	1	34	8	12	3
GNP3	434	97	5	147	0	26	21	589	708	0	182	6	19	420	22	421	0	32	2	108	33	8	13
GNP7	87	45	1	20	0	222	5	1044	265	0	38	42	5	197	91	6464	0	9	0	138	12	13	2
GNP8	118	21	1	42	0	201	9	1068	223	0	80	29	3	135	90	12114	0	10	0	70	6	15	4
GNP9	117	61	1	122	0	231	5	1224	299	0	61	34	4	145	100	9431	0	13	0	34	7	23	3
rGO3	236	76	1	135	0	54	3	252	393	0	30	2058	3	98	24	156	0	307	1	3	5	221	2
rGO4	279	155	4	1315	0	7	0	151	1907	0	1257	299	66	4518	77	14679	0	14	14	3	11	599	7
rGO5	269	230	2	1661	0	64	0	215	1035	0	1369	431	15	1618	34	2819	0	196	15	68	12	55	56
rGO6	372	212	10	668	0	13	0	557	2403	0	585	1479	169	3089	658	4440	0	17	7	6	11	146	3
rGO7	235	239	3	1416	0	0	0	95	1866	0	1360	457	111	5893	53	9714	0	15	14	17	7	35	3
rGO8	463	426	3	338	0	34	9	224	1512	0	209	1907	27	862	36	5141	0	36	3	567	52	34	12
rGO9	402	165	2	256	0	23	0	215	1505	0	235	1847	23	744	38	761	0	73	2	676	51	66	7
Amorphous Silica	3223	43	19	388	0	0	0	62	90	0	49	1	2	7669	0	3356	0	5	1	24	2	7	6
CB1	136	15	1	411	0	2	0	66	221	0	152	1	0	667	1	10799	0	5	5	2	2	29	0

XPS analysis

	XPS (atomic %)				
	C	O	N	S	Si
GNP1	96,8	3,2	0,0	0,0	0,0
GNP2	93,7	6,3	0,0	0,0	0,0
GNP3	92,4	7,6	0,0	0,0	0,0
GNP7	95,4	4,2	0,0	0,4	0,0
GNP8	93,2	5,9	0,5	0,4	0,0
GNP9	93,2	5,7	0,7	0,3	0,0
rGO3	88,1	11,9	0,0	0,0	0,0
rGO4	91,7	7,2	0,0	1,0	0,0
rGO5	96,6	2,7	0,6	0,2	0,0
rGO6	84,1	15,9	0,0	0,0	0,0
rGO7	92,6	6,7	0,0	0,7	0,0
rGO8	82,8	17,2	0,0	0,0	0,0
rGO9	95,2	2,6	2,2	0,0	0,0
Amorphous Silica	96,9	2,6	0,0	0,5	0,0
CB1	97,2	2,3	0,0	0,5	0,0

RAMAN spectra

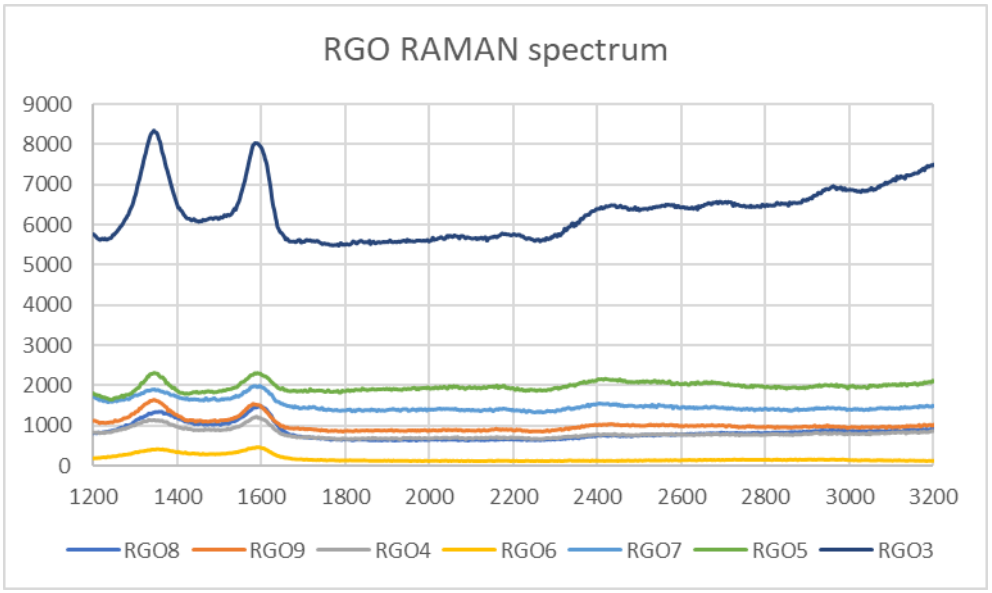

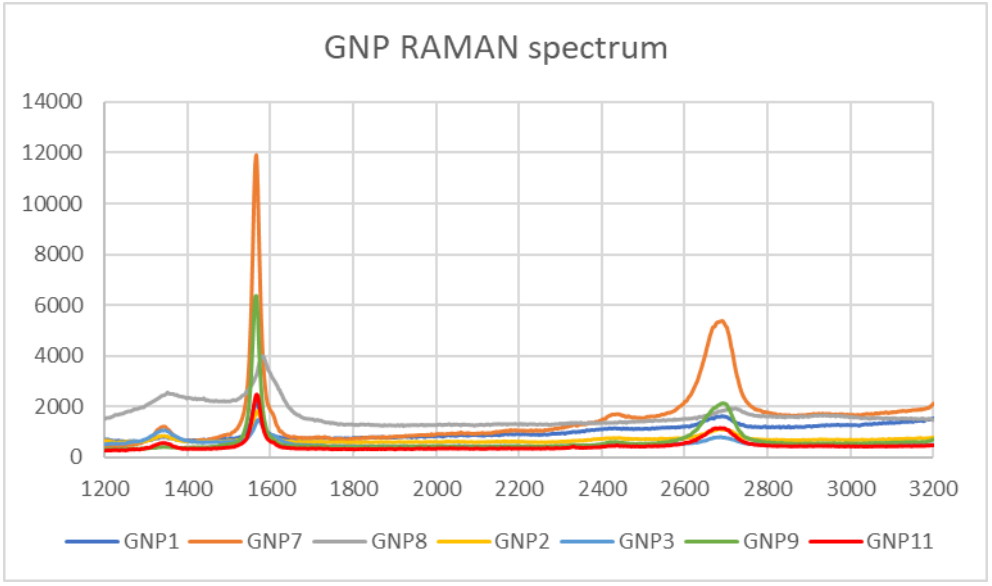

Supplementary data 2: GBMs internalization in BEAS-2B

To explore the internalization of GBMs in BEAS-2B cells, we made few acquisitions in optical and confocal microscopy.

Cell cultures were exposed to RGO4 (without metabolic activation) for 24 hours at 33.33 µg/cm² in 6-well plates Cell bind surface (Costar) maintained at 37°C in a humidified 5% CO_2 atmosphere in complete Pneumacult Ex-medium. After the beginning of exposure, cell cultures were grown for a period sufficient to undergo one mitosis and allow chromosome damage or impairment of chromosome segregation to lead to the formation of micronuclei in interphase cells. Cells were harvested, submitted to a hypotonic shock with Pneumacult Ex-medium diluted at 25% with distilled water (Versylene Fresenius), and then fixed. Giemsa stained interphase cells were then analyzed microscopically (In Cell Analyzer 6000, GE Healthcare, 60X, channel brightfiels / Channel Cy5) for the presence of micronuclei among mononucleated cells.

We selected the RGO4, one of our largest samples (mean lateral size of 31.6 µm) to make these acquisitions. For confocal microscopy, the sample was divided in 13 focal planes of 2 µm each, as shown in Figure S1. Considering that the average size of BEAS-2B is 20 µm, this allowed us to have a complete overview of the cell.

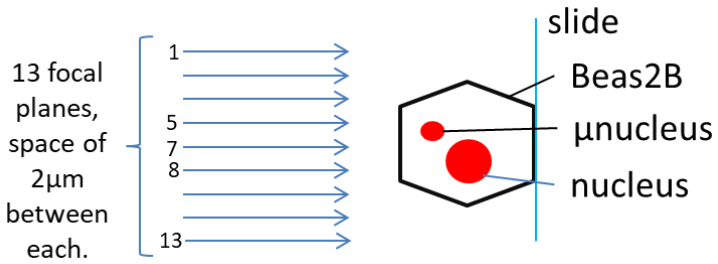

Figure S1: Focal planes for confocal microscopy.

On the first picture (Figure S2A), we can observe a BEAS-2B cell with a micronucleus and on the second picture (Figure S2B), a cell with what we assumed could be an internalized agglomerate of RGO4. We chose a focal plane approximately located in the middle of the cell and observed in Brightfield mode the cell with the micronucleus (Figure S2C) and the assumed GBM (Figure S2D). It is clear that the micronucleus is absorbing the light like the rest of the chromatin in the cell whereas the assumed GBMs remain dark. We can then confirm that we actually observe a micronucleus on Figure S2C and a GBM agglomerate on figure S2D. Lastly, we observed the two slides in confocal microscopy, on 5 different focal planes from 1 to 13 for the micronucleus sample (Figure S2E) and for the GBM sample (Figure S2F).

The micronucleus and the RGO4 agglomerate both seem to follow the same pattern through the focal planes. For that reason, it appears that the GBM is internalized in the BEAS-2B cell.

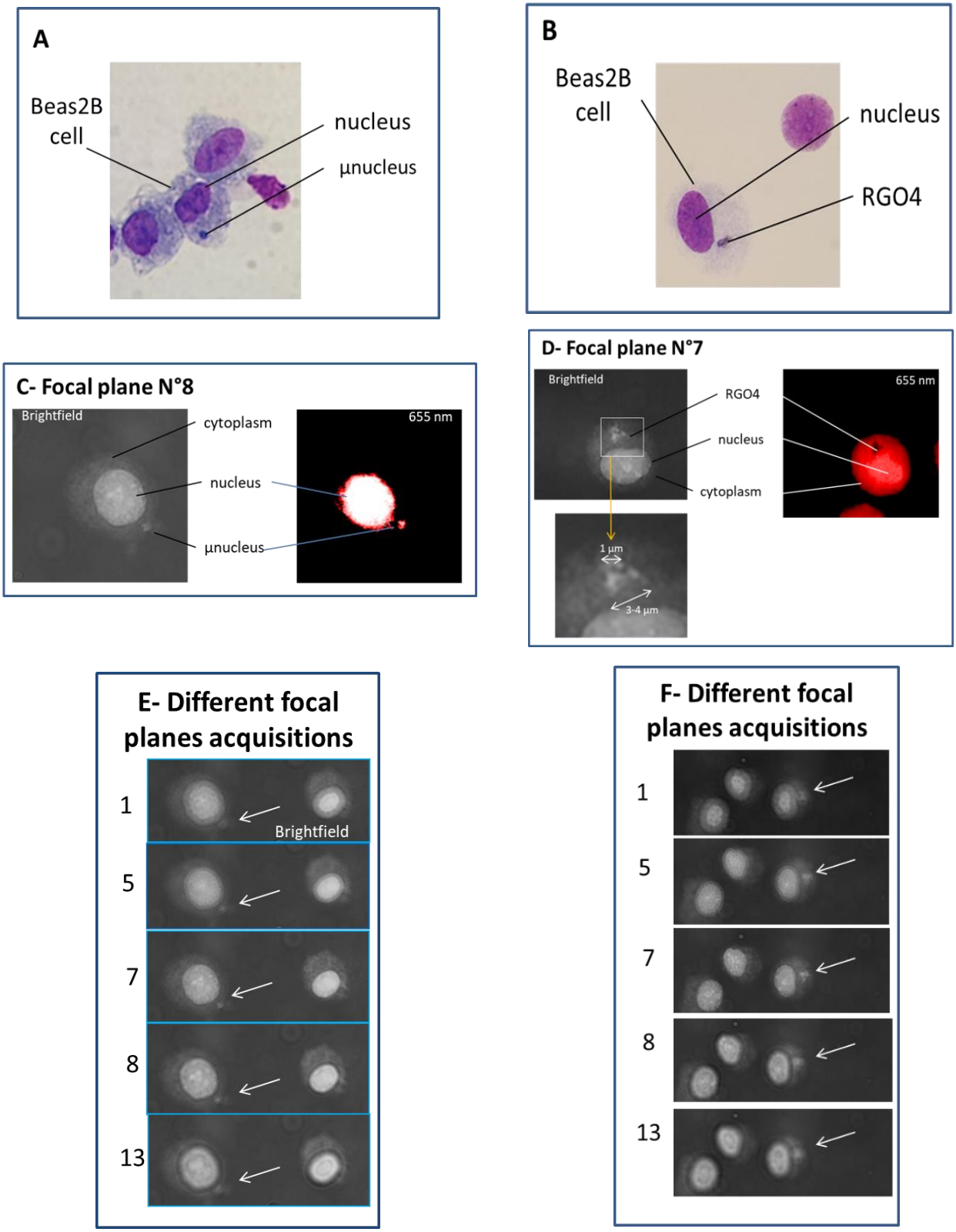

Figure S2: Confocal and optical microscopy for internalization study.
A: Optical microscopy of BEAS-2B and a micronucleus.
B: Optical microscopy of BEAS-2B and a presumed RGO4 agglomerate.
C: Focal plane number 8 (see figure 2) for BEAS-2B and micronucleus.
D: Focal plane number 7 (see figure 2) for BEAS-2B and presumed RGO4 agglomerate.
E: Different focal planes acquisitions for BEAS-2B and micronucleus.
F: Different focal planes acquisitions for BEAS-2B and presumed RGO4 agglomerate.